

We are IntechOpen, the world's leading publisher of Open Access books Built by scientists, for scientists

6,900

Open access books available

186,000

International authors and editors

200M

Downloads

Our authors are among the

154

Countries delivered to

TOP 1%

most cited scientists

12.2%

Contributors from top 500 universities



WEB OF SCIENCE™

Selection of our books indexed in the Book Citation Index
in Web of Science™ Core Collection (BKCI)

Interested in publishing with us?
Contact book.department@intechopen.com

Numbers displayed above are based on latest data collected.
For more information visit www.intechopen.com



Uncertainty Analysis Techniques Applied to Rotating Machines

Fabian Andres Lara-Molina, Arinan De Piemonte Dourado, Aldemir Ap. Cavalini Jr and Valder Steffen Jr

Abstract

This chapter presents the modeling procedure, numerical application, and experimental validation of uncertain quantification techniques applied to flexible rotor systems. The uncertainty modeling is based both on the stochastic and fuzzy approaches. The stochastic approach creates a representative model for the flexible rotor system by using the stochastic finite element method. In this case, the uncertain parameters of the rotating machine are characterized by homogeneous Gaussian random fields expressed in a spectral form by using the Karhunen-Loève (KL) expansion. The fuzzy approach uses the fuzzy finite element method, which is based on the α -level optimization. A comparative study regarding the numerical and experimental results obtained from a flexible rotor test rig is analyzed for the stochastic and fuzzy approaches.

Keywords: rotordynamics, uncertainty, fuzziness, randomness, experimental validation

1. Introduction

Rotating machines are unavoidably subjected to uncertainties that affect their parameters and, consequently, their dynamic behavior. Thus, mathematical models that encompass variability and randomness are required for the analysis and design of rotating machines instead of using deterministic models.

Uncertain dynamic responses of flexible rotors have been analyzed by applying two main approaches, namely, stochastic and fuzzy. Thus, the uncertainty analysis has been applied in flexible rotors by using the polynomial chaos theory [1], as modeled by considering Gaussian homogeneous stochastic fields discretized by Karhunen-Loève expansion [2] or through the fuzzy approach [3, 4]. These methods are well-established tools that may present limitations and drawbacks depending on the application conveyed.

In this context, this chapter presents two different approaches to model uncertain parameters and to simulate the uncertain dynamic responses of rotating machines. In this way, the stochastic and fuzzy approaches are applied to different parameters of a flexible rotor. The procedure used to obtain the stochastic model of the rotor is based on the stochastic finite element method. Moreover, the fuzzy finite element model of the rotor system is formulated according to the fuzzy approach. Then, the corresponding numerical method used to compute the fuzzy dynamic responses of the rotating machine is described. A comparative study

between the stochastic and fuzzy approaches along with the validation of the obtained results by using experimental data is presented.

2. Rotor system model

The deterministic model of a flexible rotor based on the finite element method (FE model) is obtained in this section by following the formulation previously presented in [5]. The rotor system is composed of a flexible shaft, rigid discs, and bearings. **Figure 1** shows the finite element used to represent the shaft. In this case, the finite element has two nodes and four degrees of freedom (DOFs) per node. The DOFs are associated with the nodal displacements along the x and z directions (defined by u and w , respectively) and the rotations around the x and z directions ($\theta = \partial w / \partial y$ and $\psi = \partial u / \partial y$, respectively).

In this contribution, the FE model of the shaft was obtained based on the Euler-Bernoulli and Timoshenko beam theories. The displacement field along the finite element is represented by a cubic interpolation function. Therefore, $\mathbf{u}(y, t) = \mathbf{N}(y) \mathbf{u}_e(t)$, where $\mathbf{N}(y)$ is a matrix containing shape interpolation functions and $\mathbf{u}_e(t) = [u_i \ w_i \ \theta_i \ \psi_i]^T$ ($i = 1, 2$) is the vector of DOFs.

The strain and kinetic energies of the shaft finite element are defined according to analytical equations derived from the variational principle. Therefore, the mass and stiffness elementary matrices of the shaft are given by

$$\begin{aligned} \mathbf{M}_s^e &= \int_{y=0}^L \mathbf{N}_{mi}^T(y) \mathbf{N}_{mi}(y) dy \\ \mathbf{G}_s^e &= \int_{y=0}^L \mathbf{N}_g^T(y) \mathbf{N}_g(y) dy \\ \mathbf{K}_s^e &= \int_{y=0}^L \mathbf{B}^T(y) \mathbf{E} \mathbf{B}(y) dy \end{aligned} \quad (1)$$

where \mathbf{M}_s^e ($N_e \times N_e$) is the elementary mass matrix of the shaft element, \mathbf{G}_s^e ($N_e \times N_e$) is the gyroscopic matrix, \mathbf{K}_s^e ($N_e \times N_e$) is the stiffness matrix, and \mathbf{E} is the isotropic matrix that contains the elastic properties of the material. $\mathbf{B}(y)$ is the matrix composed of differential operators that characterize the strain-displacement

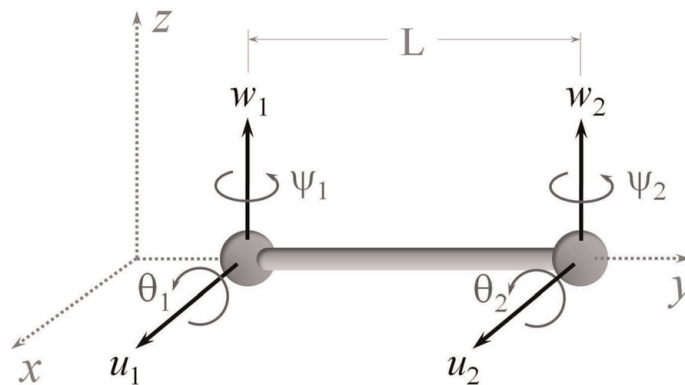


Figure 1.
Finite element of the shaft [2].

relationship. \mathbf{N}_{mi}^T and \mathbf{N}_g^T represent the shape interpolation functions associated with the mass and inertia matrices, respectively. $N_e = 8$ is the number of DOFs considered in the shaft finite element.

Rigid discs are introduced in the global FE model of the shaft by considering their corresponding kinetic energy. Thus, $\mathbf{M}_d^e (N_d \times N_d)$ and $\mathbf{G}_d^e (N_d \times N_d)$ are the mass and gyroscopic matrices associated with each disc ($N_d = y$ is the number of DOFs considered for the disc). Moreover, the bearings are modeled by using linear stiffness and damping coefficients that are introduced conveniently in the stiffness and damping matrices of the shaft FE model, respectively [6].

Eq. (2) presents the differential equation that characterizes the dynamic behavior of rotating machines (FE model with N DOFs), which is obtained by assembling the elementary finite element matrices of the shaft:

$$\mathbf{M}\ddot{\mathbf{q}}(t) + [\mathbf{C} + \Omega\mathbf{G}]\dot{\mathbf{q}}(t) + \mathbf{K}\mathbf{q}(t) = \mathbf{F}(t) \quad (2)$$

where $\mathbf{M} = \mathbf{M}_s + \mathbf{M}_d (N \times N)$ and $\mathbf{K} = \mathbf{K}_s + \mathbf{K}_b (N \times N)$ are the global mass and stiffness matrices of the rotor model, respectively. \mathbf{K}_b is the matrix containing the stiffness coefficients of the bearings. $\mathbf{C} = \mathbf{C}_b + \mathbf{C}_p (N \times N)$ is the damping matrix that considers the damping coefficients of the bearings (matrix \mathbf{C}_b) and the proportional damping $\mathbf{C}_p = \alpha\mathbf{M} + \beta\mathbf{K}$ (α and β are the so-called proportional coefficients). $\mathbf{G} = \mathbf{G}_s + \mathbf{G}_d (N \times N)$ is the gyroscopic matrix. $\mathbf{q}(t) (N \times 1)$ and $\mathbf{F}(t) (N \times 1)$ are the vectors of DOFs and external loads, respectively. Ω is the rotation speed of the shaft. More details about the formulation of the rotor FE model adopted in the present contribution can be found in [5].

3. Stochastic modeling

Among the various methods used to model uncertainties, the stochastic finite element method (SFEM) has been widely applied to complex engineering systems of industrial applications. SFEM presents well-established mathematical fundamentals and suitable experimental validation [7]. Some details about the formulation of the SFEM are presented next.

3.1 Stochastic modeling of flexible shafts

The Karhunen-Loève (KL) expansion is used to model the random fields as a spectral representation. Consequently, a random field is represented as a spatial expansion of a random variable that fluctuates randomly. For instance, uncertainties affecting Young's modulus of the shaft can be evaluated by using the KL expansion. A one-dimensional random field $H(y, \theta)$ can be defined as [8]

$$H(y, \theta) = E(y) + \sum_{r=1}^{n_{KL}} \sqrt{\lambda_r} f_r(y) \xi_r(\theta) \quad (3)$$

where $f_r(y)$ and λ_r are the eigenfunctions and eigenvalues of the covariance function $C(y_1, y_2)$, respectively. n_{KL} is the number of terms used in the KL expansion.

In this work, the exponential covariance is adopted, which is defined as $C(y_1, y_2) = e^{(-|y_1 - y_2|/L_c)}$, where $(y_1, y_2) \in [0, L]$ and L_c represent the correlation length. $\xi_r(\theta)$ denotes the random variables that are orthonormal with respect to the functions $f_r(y)$. The KL expansion is used to model the stochastic finite element matrices of the flexible shaft, as given by Eq. (4):

$$\begin{aligned}\mathbf{M}_s^e(\theta) &= \mathbf{M}_s + \sum_{r=1}^{n_{KL}} \bar{\mathbf{M}}_{sr}^e \xi_r(\theta) \\ \mathbf{K}_s^e(\theta) &= \mathbf{K}_s + \sum_{r=1}^{n_{KL}} \bar{\mathbf{K}}_{sr}^e \xi_r(\theta) \\ \mathbf{G}_s^e(\theta) &= \mathbf{G}_s + \sum_{r=1}^{n_{KL}} \bar{\mathbf{G}}_{sr}^e \xi_r(\theta)\end{aligned}\tag{4}$$

where \mathbf{M}_s , \mathbf{K}_s , and \mathbf{G}_s are the deterministic elementary mass, stiffness, and gyroscopic matrices of the shaft, respectively. The stochastic matrices are obtained by solving the following expressions:

$$\begin{aligned}\bar{\mathbf{M}}_{sr}^e &= \int_{y=0}^L \sqrt{\lambda_r} f_r(y) \mathbf{N}_{mi}^T(y) \mathbf{N}_{mi}(y) dy \\ \bar{\mathbf{K}}_{sr}^e &= \int_{y=0}^L \sqrt{\lambda_r} f_r(y) \mathbf{B}^T(y) \bar{\mathbf{E}} \mathbf{B}(y) dy \\ \bar{\mathbf{G}}_{sr}^e &= \int_{y=0}^L \sqrt{\lambda_r} f_r(y) \mathbf{N}_g^T(y) \mathbf{N}_g(y) dy\end{aligned}\tag{5}$$

in which $\bar{\mathbf{E}}$ is the mechanical property matrix that contains the parameters E_s , A_s , and I_s (Young's modulus, cross-sectional area, and inertia moment of the shaft, respectively).

3.2 Stochastic modeling of bearings' parameters

The uncertainties associated with bearings' stiffness and damping coefficients of rotating machines can be evaluated by using the following relations: $k(\theta) = k_o + k_o \delta_k \xi(\theta)$ and $d(\theta) = d_o + d_o \delta_d \xi(\theta)$, respectively. In this case, k_o and d_o are the mean values of the stiffness and damping coefficients of the bearings, respectively. δ_k and δ_d are the corresponding dispersion levels. $\xi(\theta)$ represents the stochastic distribution. The stochastic model of the rotor is solved by using the Monte Carlo simulation (MCS) in combination with Latin hypercube sampling [9].

3.3 Numerical results

In this section, SFEM is applied to the FE model as given by **Figure 2**. The rotating machine is composed of a horizontal flexible shaft discretized into 20 Euler-Bernoulli's beam elements, three asymmetric bearings (B_1 , B_2 , and B_3), and two rigid discs (D_1 and D_2). The physical and geometrical characteristics used in the FE model of the rotor system are given in [2].

In this case, the uncertain random fields associated with Young's modulus of the shaft are modeled as homogeneous Gaussian stochastic fields, which are represented in the spectral form by using the Karhunen-Loève expansion. The uncertainty variables associated with the stiffness and damping coefficients of the

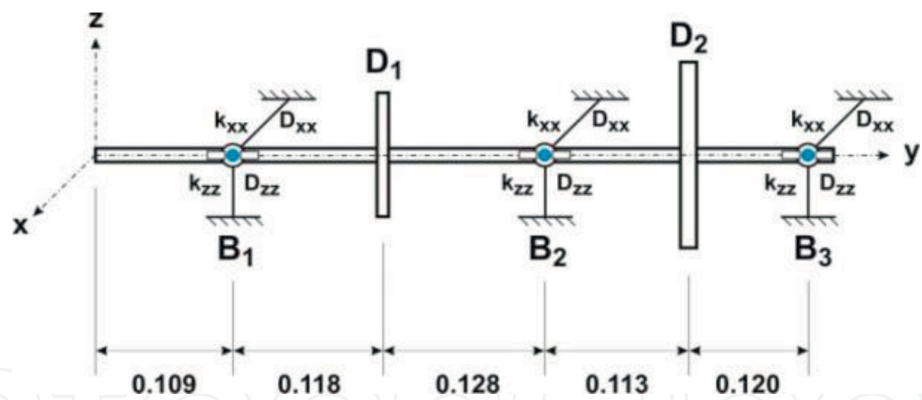


Figure 2.
Numerical model of the flexible rotor system [2].

Scenario	n_{KL}	n_s
(a)	$1 \leq n_{KL} \leq 50$	100
(b)	10	$1 \leq n_s \leq 250$

Table 1.
Parameters of convergence analysis simulation.

bearings are modeled as random variables. This modeling process considers the frequency- and time-domain vibration responses of the rotating machine in terms of their working envelopes (frequency response functions (FRFs) and orbits). Initially, the convergence of the stochastic model is verified by changing the number of terms used in the KL expansion and the number of samples considered in MCS (n_{KL} and n_s , respectively). The convergence analysis was performed based on the root-mean-square (RMS) value as given by Eq. (6):

$$RMS = \left[\frac{1}{n_s} \sum_{j=1}^{n_s} |\mathbf{H}_j(\omega, \Omega, \theta) - \mathbf{H}_j(\omega, \Omega)|^2 \right]^{\frac{1}{2}} \tag{6}$$

where $\mathbf{H}(\omega, \Omega)$ is the FRF obtained by using the deterministic FE model of the rotor and $\mathbf{H}(\omega, \Omega, \theta)$ is the corresponding FRF of the stochastic model associated with independent realizations θ . In this case, ω is the frequency. The deterministic and stochastic FRFs were obtained by considering the shaft at rest ($\Omega = 0$) from impacts performed along the x direction of the disc D_1 and measures obtained at the same position and direction. Two scenarios were evaluated to achieve convergence for n_{KL} and n_s , as given by **Table 1**. In both cases, the correlation length L_C was assumed as being equal to the length of the shaft elements.

Figures 3a and **b** present the upper and lower limits of the RMS envelopes obtained by considering the scenarios (a) and (b) of **Table 1**, respectively. Note that convergence is achieved for $n_{KL} = 10$ and $n_s = 70$.

Figure 4a and **b** show the FRF and orbit, respectively, obtained by using the deterministic (mean) and stochastic FE models of the rotor system. The uncertain envelopes were determined by applying a 5% dispersion level both in Young's modulus of the shaft (E_s) and in the stiffness and damping coefficients of the bearings (k_{xx} , k_{zz} , d_{xx} , and d_{zz} ; see **Figure 2**). The results show the influence of the uncertain parameters on the dynamic behavior of the flexible rotor, which are highlighted by the dispersion of the uncertain envelopes around the curves of the deterministic FRF and orbit (mean model) (**Figures 3** and **4**).

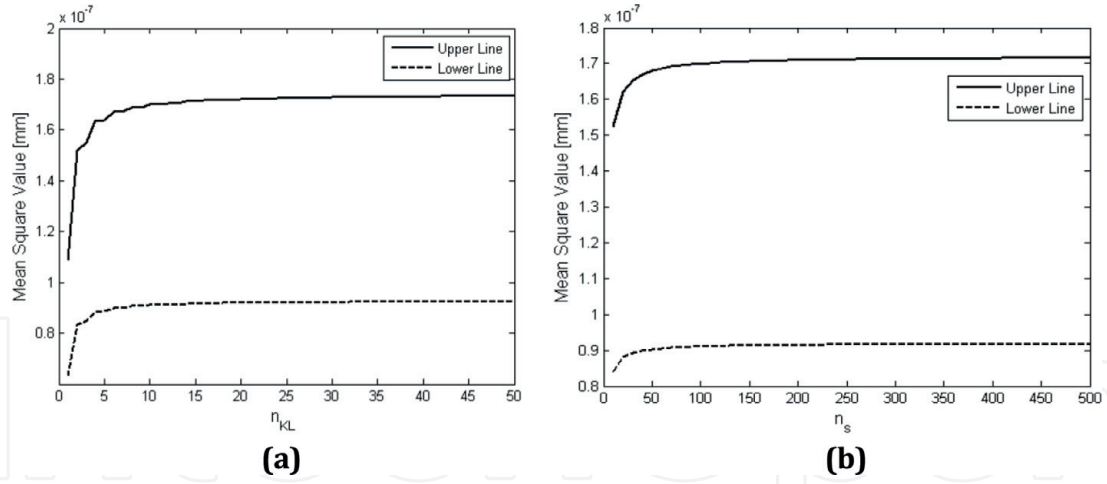


Figure 3.
Convergence simulation: (a) n_{KL} and (b) n_s [2].

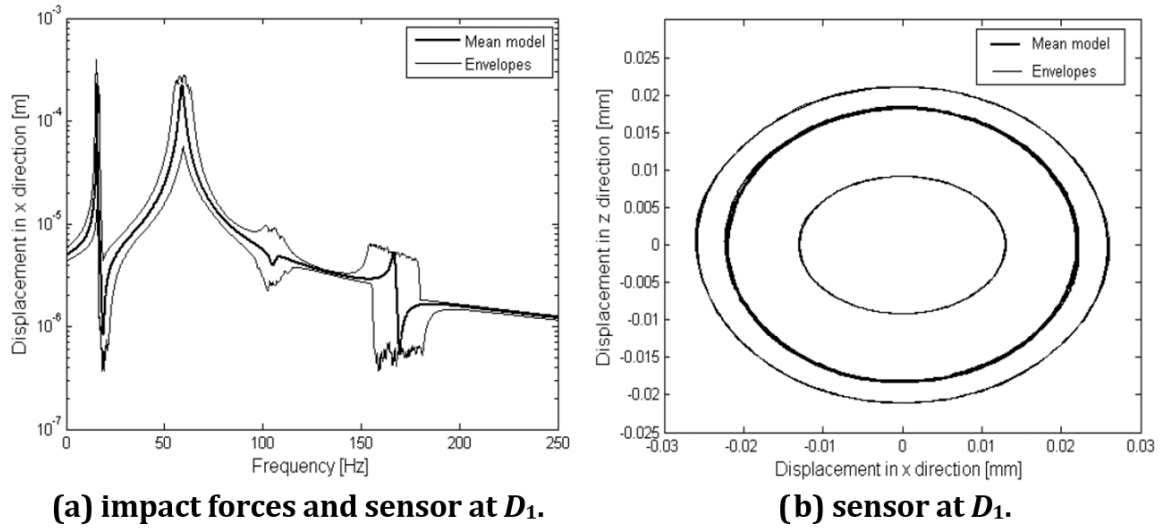


Figure 4.
Stochastic responses: (a) FRF and (b) orbits [2].

4. Fuzzy dynamic analysis

The fuzzy dynamic analysis computes the uncertain dynamic responses of rotating machines by modeling the uncertain parameters as fuzzy variables or fuzzy fields. The fuzzy dynamic analysis is based on the α -level optimization, which was introduced by [10]. In the α -level approach, an optimization problem should be solved to compute the fuzzy responses of the system as presented next.

4.1 Fuzzy variables

Figure 5 presents the definition of fuzzy sets. Considering \mathbf{X} as a universal set whose elements are defined by x , subset A ($A \in \mathbf{X}$) is defined by the membership function $\mu_A: \mathbf{X} \rightarrow \{0, 1\}$, where μ_A is a membership function with real value and continuous interval. Each element belongs (for $\mu_A = 1$) or does not belong to the classical set A (see **Figure 5a**). Moreover, a fuzzy set \tilde{A} is defined by the membership function $\mu_A: \mathbf{X} \rightarrow [0, 1]$. The membership function $\mu_A(x)$ defines how compatible the element x is with respect to the fuzzy set \tilde{A} . Thus, $\mu_A(x)$ close to 1 indicates high pertinence of x to \tilde{A} .

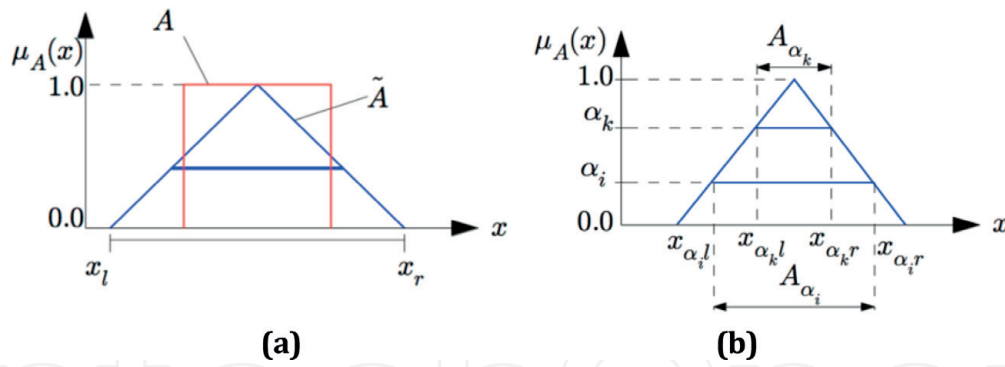


Figure 5.
 Fuzzy set: (a) definition and (b) α -level representation [11].

Fuzzy variables are represented by using intervals weighted by the membership function, namely, α -levels. According to the α -level representation, \tilde{A} is defined as

$$\tilde{A} = \{(x, \mu_A(x)) | x \in \mathbf{X}\} \quad (7)$$

where $0 \leq \mu_A(x) \leq 1$.

Moreover, according to **Figure 5b**

$$\tilde{A}_{\alpha_k} = \{x \in \mathbf{X}, \mu_A(x) \geq \alpha_k\} \quad (8)$$

If the fuzzy set is convex, each α -level subset A_{α_k} corresponds to the interval $[x_{\alpha_k l}, x_{\alpha_k u}]$, where

$$\begin{aligned} x_{\alpha_k l} &= \min [x \in \mathbf{X}, \mu_A(x) \geq \alpha_k] \\ x_{\alpha_k u} &= \max [x \in \mathbf{X}, \mu_A(x) \geq \alpha_k] \end{aligned} \quad (9)$$

4.2 Fuzzy dynamic analysis

The fuzzy dynamic analysis is a numerical method used to map a fuzzy input \tilde{x} onto a fuzzy output $\tilde{z}(\tau)$ by using deterministic models, as given by Eq. (2). Thus, the fuzzy finite element method is defined by combining fuzzy parameters (uncertain information) with a deterministic model based on the classic FE method.

Figure 6 shows that the fuzzy dynamic analysis is composed of two main steps. The first step consists in discretizing the input fuzzy parameter according to the α -level representation presented in Eq. (8) and **Figure 5b**. Thus, each fuzzy parameter of the vector $\tilde{x} = (\tilde{x}_1, \dots, \tilde{x}_n)$ is represented by an interval $X_{iak} = [x_{iakl}, x_{iaku}]$, where $\alpha_k \in [0, 1]$. Therefore, the subspace crisp \underline{X}_{α_k} is defined as $\underline{X}_{\alpha_k} = (X_{1\alpha_k}, \dots, X_{n\alpha_k}) \in \mathbb{R}^n$.

In the second step, an optimization problem is performed. This optimization process maximizes and minimizes the value of the output for the mapping model $M : \underline{z} = f(\underline{x})$ and over the subspace crisp at each evaluated value τ . Thus,

$$\begin{aligned} z_{\alpha_k l} &= \min_{\underline{x} \in \underline{X}_{\alpha_k}} f(\underline{x}, \tau) \\ z_{\alpha_k u} &= \max_{\underline{x} \in \underline{X}_{\alpha_k}} f(\underline{x}, \tau) \end{aligned} \quad (10)$$

where $z_{\alpha_k l}$ and $z_{\alpha_k u}$ are the lower and upper limits of the interval $z_{\alpha_k} = [z_{\alpha_k l}, z_{\alpha_k u}]$ corresponding to the α -level α_k .

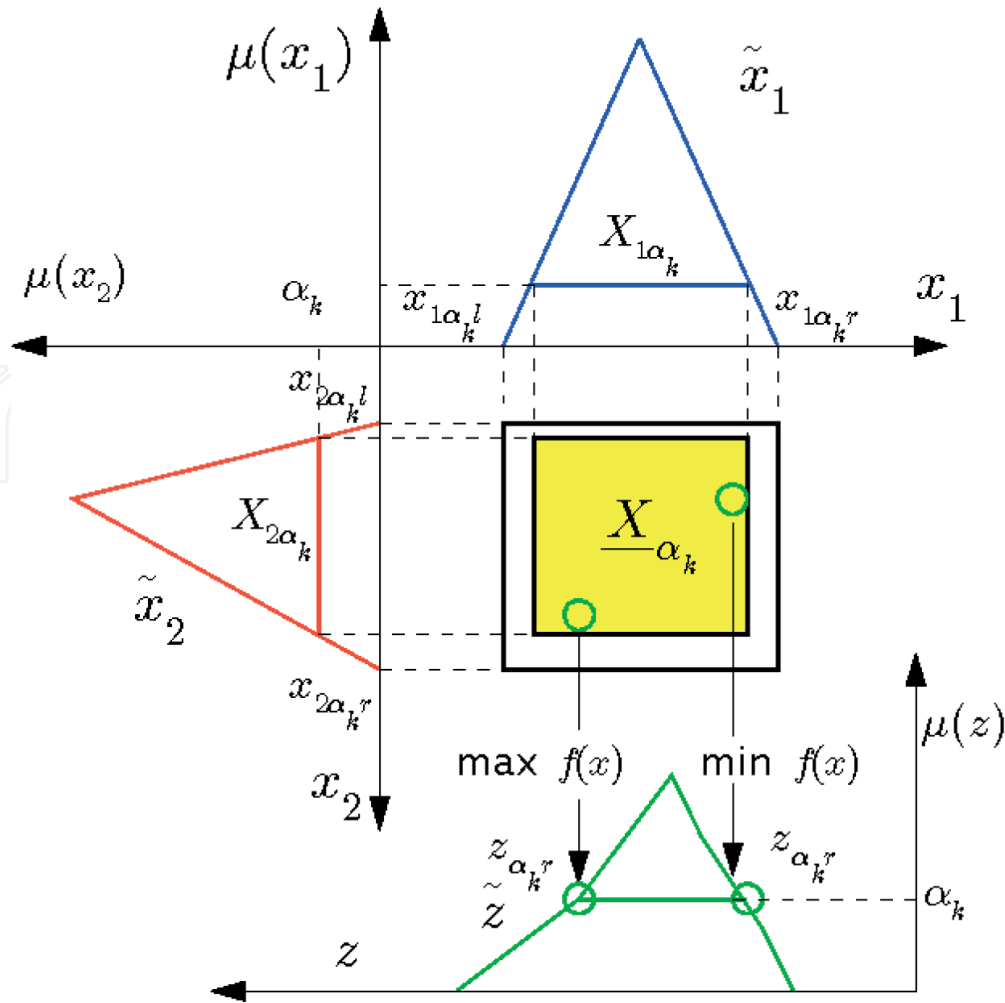


Figure 6.
 α -Level optimization.

The complete set of the intervals z_{α_k} for $\alpha_k \in [0, 1]$ forms the fuzzy resulting variable $\tilde{z}(\tau)$ evaluated at τ .

The fuzzy analysis of either a transient time-domain response or a frequency response function demands the solution of a large number of α -level optimization processes, i.e., one α -level optimization at each considered time or frequency step. In the present contribution, the optimization associated with the α -levels is solved by using the differential evolution optimization algorithm [12].

4.3 Numerical results

The numerical results for the fuzzy analysis are also obtained by using the rotor FE model presented in **Figure 2**. In this case, Young's modulus E_s of the shaft and the stiffness and damping coefficients of the bearings (B_1 , B_2 , and B_3) were considered as fuzzy triangular numbers (uncertain parameters). In this case, a 5% dispersion level was applied around the deterministic value of Young's modulus and a 15% dispersion level around the deterministic values of the stiffness and damping coefficients of the bearings. The fuzzy response of the rotor system was assessed at three different α -levels: 0, 0.5, and 1.0. **Figure 7a** and **b** shows the FRF and orbit obtained by applying the fuzzy uncertain analysis technique, respectively.

The fuzzy responses both on the time and frequency domains show that the fuzzy uncertainty parameters produce a significant variation of the lower and upper curves of the fuzzy envelope. Note that the results obtained in the present analysis are similar to the ones presented in **Figure 4**, for which the stochastic approach was applied.

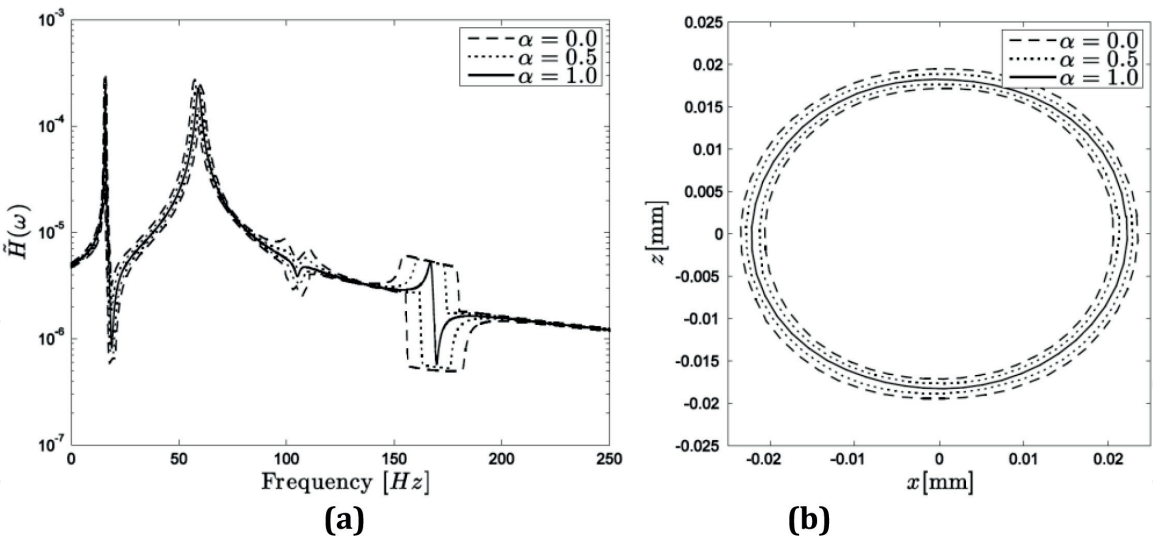


Figure 7.
Fuzzy responses: (a) FRF and (b) orbit [3].

5. Comparative study of uncertainty quantification techniques

The uncertainty analysis of dynamic systems has been previously studied by applying techniques based both on stochastic and fuzzy approaches. The fuzzy approach has demonstrated to be more appropriate in the cases of applications for which there is no knowledge regarding the stochastic process that governs the uncertainties themselves.

In the present study, the uncertainties that affect the dynamic response of a flexible rotor system are modeled by using both stochastic and fuzzy approaches. These methodologies have been compared by evaluating the dynamic responses obtained by numerical simulations regarding the frequency responses and time-domain responses. The numerical and experimental results of this section have been obtained from the flexible rotor test rig depicted in **Figure 8**.

The corresponding FE model was discretized in 33 finite elements, as given by **Figure 8b**. This rotating machine is composed of a flexible steel shaft of 860 length and 17 mm diameter ($E = 205$ GPa, $\rho = 7850$ kg/m³, $\nu = 0.29$); two ball bearings (B_1 and B_2); located at nodes #4 and #31, respectively; and two rigid discs D_1 (located at node #13) and D_2 (at node #23). Displacement sensors are placed at nodes #8 (S_{8X} and S_{8Z}) and #28 (S_{28X} and S_{28Z}) to measure the shaft vibration responses. An electric DC motor drives the shaft.

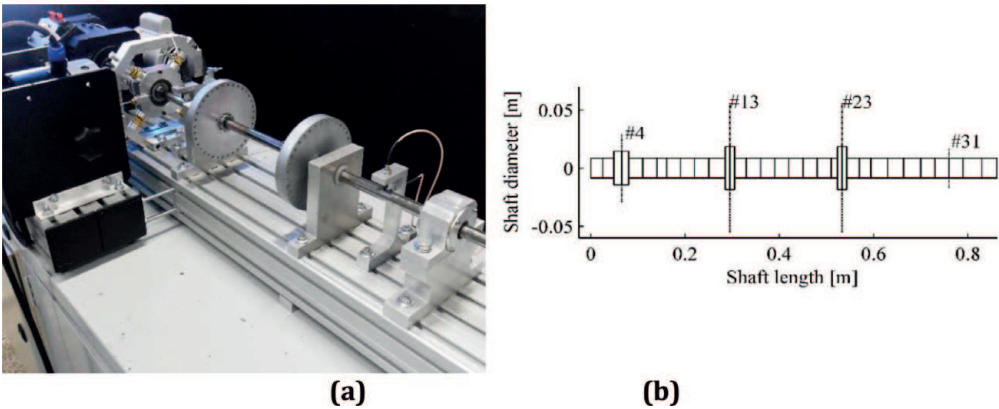


Figure 8.
Experimental rotor: (a) test rig and (b) FE model [13].

A representative FE model of the rotating machine was obtained by applying a model updating procedure. The differential evolution optimization approach was used to identify the unknown parameters of the FE model, namely, coefficients α and β (proportional damping), the stiffness and damping coefficients of the bearings, and the angular stiffness k_{ROT} introduced by the coupling between the electric motor and the shaft (orthogonal to plane XZ at node #1). Further information about the model updating procedure can be found in [8].

Figure 9 shows the simulated Bode diagram obtained by using the parameters identified by the considered optimization procedure. The experimental diagram is added to the figure for comparison purposes. The similarity between the numerical and experimental Bode diagrams demonstrates the representativeness of the obtained FE model.

5.1 Frequency-domain analysis

In the present analysis, the uncertain envelope of the FRF was obtained by considering Young's modulus of the shaft as uncertain information. Regarding the stochastic approach, uncertain Young's modulus is modeled as a Gaussian random field with nominal value $E_s = 205$ GPa and a 15% dispersion level. The convergence analysis was carried out to evaluate the number of terms retained in the truncated KL expansion (n_{KL}) and the number of samples for MCS (n_S). The RMS convergence analysis for the realizations of the FRF is assessed according to Eq. (6).

Figure 10 presents the obtained results. Note that convergence was achieved for $n_{KL} = 40$ and $n_S = 250$.

For the fuzzy approach, a fuzzy triangular number with the same nominal value and dispersion considered for the stochastic approach ($\tilde{E}_S = 205 \pm 15\%$ GPa) is used. The objective function of the α -level optimization is the norm of the FRF.

In this contribution, the performed uncertainty analysis aims at obtaining the minimum and maximum responses of the rotor system, i.e., the bounds of the uncertain dynamic responses. Therefore, the fuzzy uncertainty analysis was devoted to the α -level, $\alpha_k = 0$. Thus, the dynamic responses of the rotor are obtained

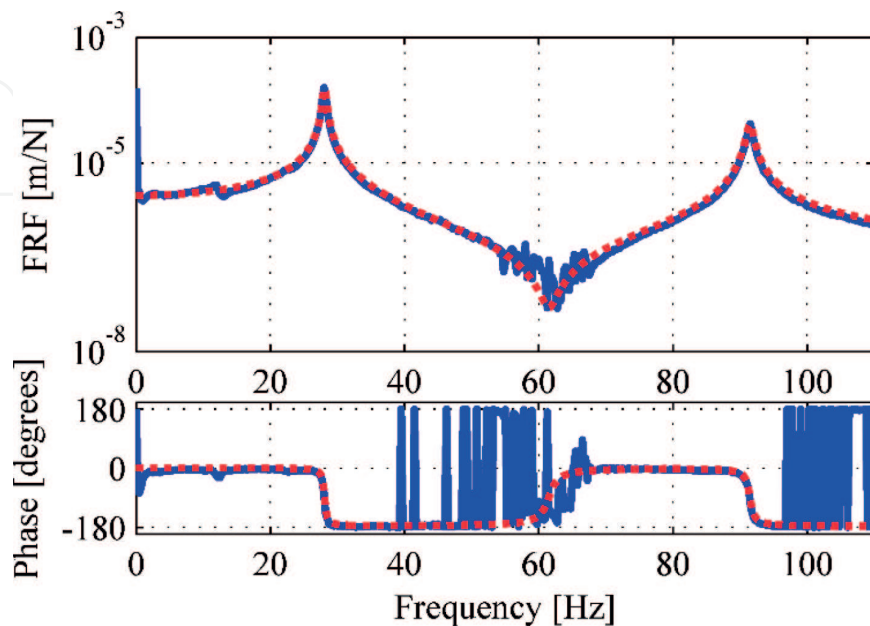


Figure 9. Simulated (—) and experimental (—) Bode diagrams obtained from impact forces applied at D_1 and the sensor S_{8X} [13].

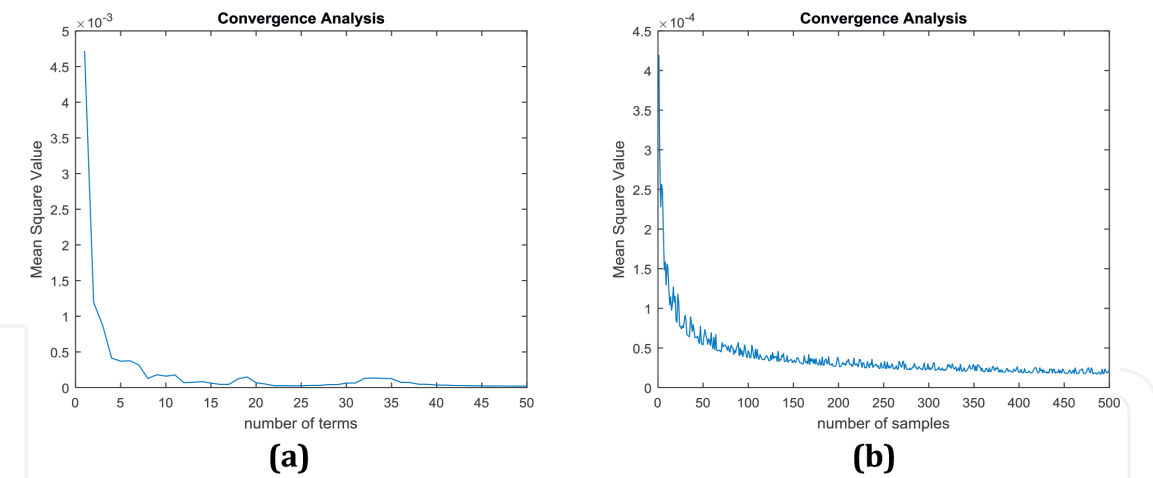


Figure 10.
Convergence analysis for the FRF: (a) n_{KL} and (b) n_s [13].

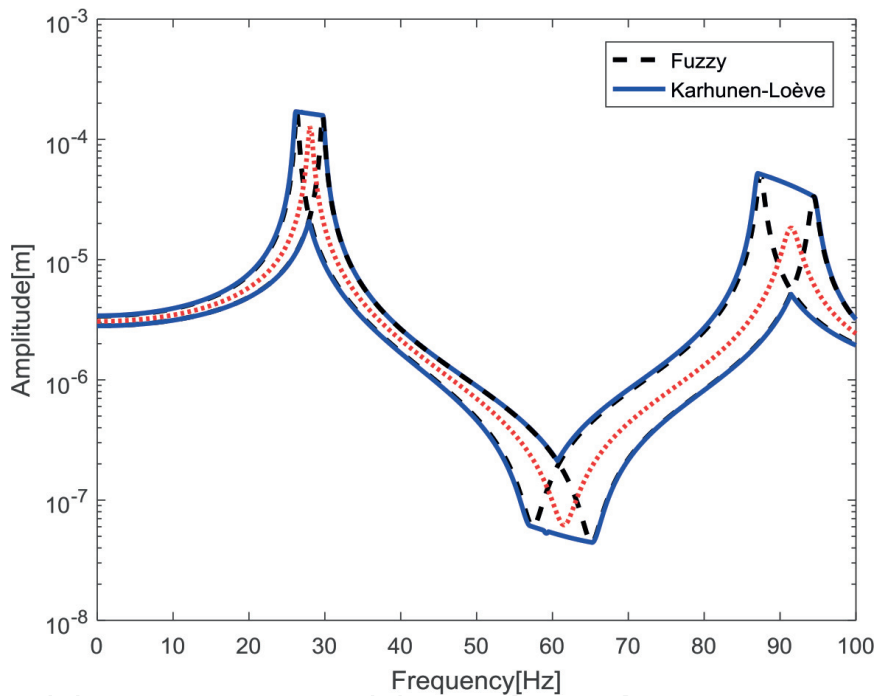


Figure 11.
FRFs obtained by using the stochastic and fuzzy approaches [13].

by considering the maximum level of uncertainty. Moreover, the stochastic approach is also applied to compute the minimum and maximum dynamic responses of the rotor.

Figure 11 presents a comparative evaluation of the FRFs' uncertain envelopes obtained by applying the stochastic and fuzzy approaches. In this case, the obtained FRFs were determined by considering the force applied along the x direction of disc D_1 and sensor S_{8X} . The results show that the uncertain envelopes obtained from the stochastic and fuzzy approaches are similar. Additionally, the updated FRF is also shown for comparison purposes.

5.2 Time-domain analysis

The time-domain analysis was performed based on the orbits of the flexible shaft. This analysis considers uncertainties affecting the stiffness coefficients k_{xx}

and k_{zz} of bearing B_1 . For the stochastic approach, the uncertain parameters were modeled as Gaussian random variables with $k_{xx} = 8.551 \times 10^5$ N/m, $k_{zz} = 1.198 \times 10^6$ N/m (mean values), and deviation of $\pm 10\%$. The rotation speed of the rotor is 1200 rev/min, and an unbalance of 487.5 g mm/ 0° was applied to disc D_1 .

The convergence analysis was performed to determine n_{KL} and n_s based on the time-domain vibration responses of the rotor system. **Figure 12** shows the obtained results. Note that convergence was achieved for $n_{KL} \geq 100$ and $n_s \geq 500$.

Considering the fuzzy approach, the uncertain parameter is defined as a fuzzy triangular number with the same nominal value and deviation of the stochastic modeling. The objective function of the α -level optimization is written as the norm of the shaft displacement measured by sensor S_{8X} . **Figure 13** presents a comparative

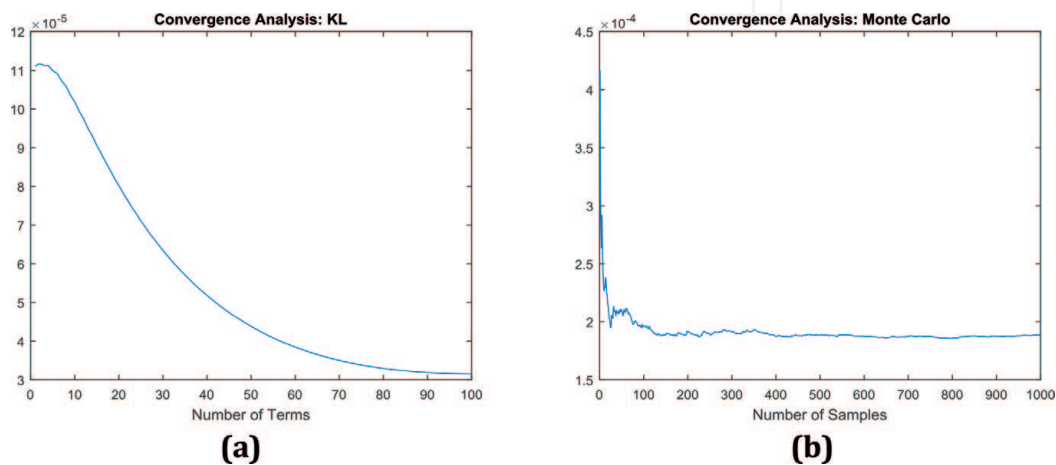


Figure 12.
Convergence analysis for the orbits: (a) n_{KL} and (b) n_s [13].

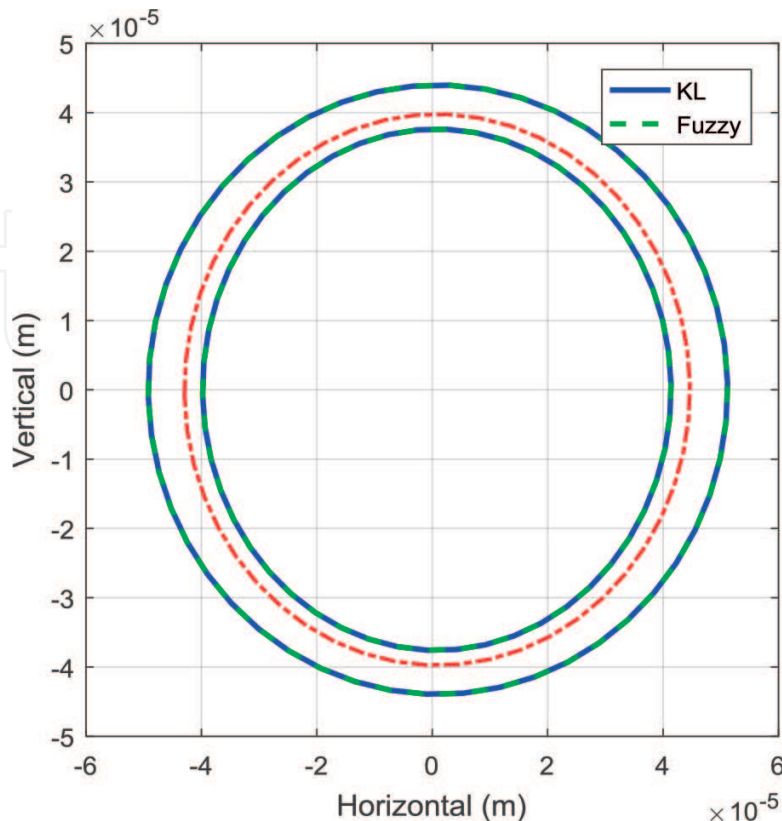


Figure 13.
Orbits obtained by using both the stochastic and fuzzy approaches [13].

evaluation of the uncertain envelopes of the rotor orbits determined by using the stochastic and fuzzy approaches. Note that the obtained results are similar, demonstrating that both approaches lead to equivalent responses.

6. Conclusions

This chapter is dedicated to the modeling, numerical methods, and simulations for the uncertainty analysis of flexible rotors. The stochastic and fuzzy approaches showed to be suitable methods to quantify the effect of uncertain parameters on the dynamic responses of rotating machines. The comparative study permitted to evaluate the two studied approaches is based on numerical simulations. Although the numerical results obtained by applying both approaches were similar, the fuzzy approach demands a greater computational effort than the stochastic method. Nevertheless, the stochastic approach requires an extensive mathematical background and an insight knowledge on the uncertain parameters. In this case, the stochastic distribution should be known or assumed. However, both approaches can be applied to the design of rotating machines.

Acknowledgements

The authors are thankful for the financial support provided to the present research effort by CNPq (574001/2008-5, 304546/2018-8, and 431337/2018-7), FAPEMIG (TEC-APQ-3076-09, TEC-APQ-02284-15, TEC-APQ-00464-16, and PPM-00187-18), and CAPES through the INCT-EIE. The authors are also thankful to the companies CERAN, BAESA, ENERCAN, and Foz do Chapecó for the financial support through the R&D project Robust Modeling for the Diagnosis of Defects in Generating Units (02476-3108/2016).

Author details

Fabian Andres Lara-Molina¹, Arinan De Piemonte Dourado²,
Aldemir Ap. Cavalini Jr³ and Valder Steffen Jr^{3*}

1 Mechanical Engineering Department, Federal University of Technology-Paraná,
Cornélio Procópio, Brazil

2 Department of Mechanical and Aerospace, Engineering Probabilistic Mechanics
Laboratory, University of Central Florida, Orlando, FL, USA

3 LMEst – Structural Mechanics Laboratory, Federal University of Uberlândia,
School of Mechanical Engineering, Brazil

*Address all correspondence to: vsteffen@ufu.br

IntechOpen

© 2019 The Author(s). Licensee IntechOpen. This chapter is distributed under the terms of the Creative Commons Attribution License (<http://creativecommons.org/licenses/by/3.0>), which permits unrestricted use, distribution, and reproduction in any medium, provided the original work is properly cited. 

References

- [1] Didier J, Faverjon B, Sinou JJ. Analyzing the dynamic response of a rotor system under uncertain parameters by polynomial chaos expansion. *Journal of Vibration and Control*. 2012;**18**(5):587-607
- [2] Koroishi EH, Cavalini AA Jr, de Lima AM, Steffen V Jr. Stochastic modeling of flexible rotors. *Journal of the Brazilian Society of Mechanical Sciences and Engineering*. 2012;**34** (SPE2):574-583
- [3] Lara-Molina FA, Koroishi EH, Steffen V Jr. Uncertainty analysis of flexible rotors considering fuzzy parameters and fuzzy-random parameters. *Latin American Journal of Solids and Structures*. 2015;**12**(10): 1807-1823
- [4] Cavalini AA, Silva ADG, Lara-Molina FA, Steffen V. Dynamic analysis of a flexible rotor supported by hydrodynamic bearings with uncertain parameters. *Meccanica*. 2017;**52**(11-12):2931-2943
- [5] Lalanne M, Ferraris G. *Rotordynamics—Prediction in Engineering*. New York: John Wiley & Sons; 1998
- [6] Maia NMM, Montalvão e Silva JM. *Theoretical and Experimental Modal Analysis*. England: Research Studies Press LTD.; 1997. 468 p
- [7] Soize C. Stochastic modeling of uncertainties in computational structural dynamics—Recent theoretical advances. *Journal of Sound and Vibration*. 2013;**332**(10):2379-2395
- [8] Ghanem RG, Spanos PD. Stochastic finite element method: Response statistics. In: *Stochastic Finite Elements: A Spectral Approach*. New York, NY: Springer; 1991. pp. 101-119
- [9] Florian A. An efficient sampling scheme: updated Latin hypercube sampling. *Probabilistic Engineering Mechanics*. 1992;**7**(2):123-130
- [10] Möller B, Beer M. *Fuzzy Randomness: Uncertainty in Civil Engineering and Computational Mechanics*. Springer Science & Business Media; 2013
- [11] Cavalini AA, Silva AG, Lara-Molina FA, Steffen V. Uncertainty analysis of a tilting-pad journal bearing using fuzzy logic techniques. *Journal of Vibration and Acoustics*. 2016;**138**(6):061016
- [12] Price KV, Storn RM, Lampinen JA. *Differential Evolution: A Practical Approach to Global Optimization*. Berlin, Germany: Springer-Verlag; 2005
- [13] Silva ADG, Cavalini AA, Steffen V. Uncertainty quantification techniques applied to rotating systems: A comparative study. *Journal of Vibration and Control*. 2017;**1**(1):1-16